STRUCTURAL BASES OF ATYPICAL WHISKER RESPONSES IN A MOUSE MODEL OF CDKL5 DEFICIENCY DISORDER

R. Pizzo[1], A. Lamarca[1,a], M. Sassoè-Pognetto[1,2], M. Giustetto[1,2]

[1]Department of Neuroscience, University of Turin, Corso Massimo D'Azeglio 52, 10126 Turin, Italy
[2]National Institute of Neuroscience-Italy, Corso Massimo D'Azeglio 52, 10126 Turin, Italy
[a] Present address: Cell Adhesion Unit, San Raffaele Scientific Institute, Via Olgettina 60, 20132 Milan, Italy

Corresponding author contact information:

Prof. Maurizio Giustetto

Dipartimento di Neuroscienze, Università di Torino

Corso M. D'Azeglio 52, 10126 TORINO (Italy).

Email: maurizio.giustetto@unito.it

Graphical Abstract

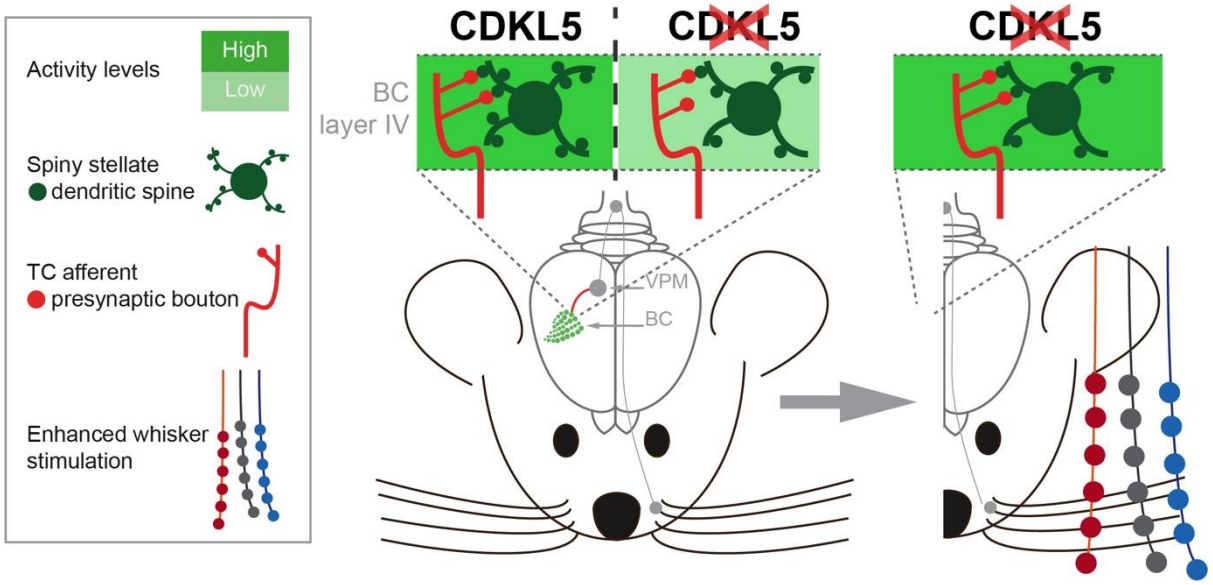

Highlights

- CDKL5 deficiency disrupts the synaptic organization of thalamo-cortical (TC) and cortico-cortical (CC) connections in the barrel cortex (BC)
- CDKL5 deficiency leads to BC hypoactivation
- CDKL5 deficiency causes atypical whisker-mediated behavioural responses
- CDKL5 deficiency does not prevent TC circuitry to undergo experience-dependent structural plasticity
- Enhanced sensory stimulation restores cortical connectivity, BC activation levels and whisker-related behavioural responses

ABSTRACT

Mutations in the *CDKL5* (cyclin-dependent kinase-like 5) gene cause CDKL5 Deficiency Disorder (CDD), a severe neurodevelopmental syndrome where patients exhibit early-onset seizures, intellectual disability, stereotypies, limited or absent speech, autism-like symptoms and sensory impairments. Mounting evidences indicate that disrupted sensory perception and processing represent core signs also in mouse models of CDD, however we have very limited knowledge on their underlying causes. In this study, we investigated how CDKL5 deficiency affects synaptic organization and experience-dependent plasticity in the thalamo-cortical (TC) pathway carrying whisker-related tactile information to the barrel cortex (BC). By using synapse-specific antibodies and confocal microscopy, we found that Cdkl5-KO mice display a lower density of TC synapses in the BC that was paralleled by a reduction of cortico-cortical (CC) connections compared to wild-type mice. These synaptic defects were accompanied by reduced BC activation, as shown by a robust decrease of c-fos immunostaining, and atypical behavioural responses to whisker-mediated tactile stimulation. Notably, a two-day paradigm of enriched whisker stimulation rescued both number and configuration of TC and CC synapses in Cdkl5-KO mice, and restored cortical activity as well as behavioural responses to control levels. Our findings disclose an important role of CDKL5 in controlling the organization and experience-induced modifications of excitatory connections in the BC and indicate how mutations of CDKL5 produce failures in higher-order processing of somatosensory stimuli.

Keywords

Rett Syndrome, barrel cortex, thalamo-cortical, synaptic plasticity.

INTRODUCTION

De novo mutations of the Cyclin-dependent kinase-like 5 (*CDKL5*) gene lead to a rare X-linked genetic disorder (Weaving et al., 2004). CDKL5 deficiency disorder (CDD) patients exhibit among a broad spectrum of clinical signs severe deficits in motor coordination, abnormalities in tactile and visual perception, and autistic traits. In CDD individuals, defective sensory processing in primary cortical areas is thought to be involved in the loss of purposeful hands movement and the progressive appearance of dyspraxia or apraxia, until walking is completely prevented (Bahi-Buisson and Bienvenu, 2011). Sensory defects such visual and auditory impairments were recently revealed in CDD mouse models (Wang et al., 2012; Amendola et al., 2014; Trazzi et al., 2016; Mazziotti et al., 2017). Moreover, CDD mouse models exhibit autistic-like features such as profoundly altered social interaction (Wang et al., 2012; Jhang et al., 2017; Yennewar et al., 2019).

CDKL5 mouse models offer a valuable opportunity to assess the cellular and molecular mechanisms underlying abnormal computation of sensory inputs in CDD (Wang et al., 2012; Amendola et al., 2014; Trazzi et al., 2016; Mazziotti et al., 2017). CDKL5 is a serine/threonine kinase that is highly expressed in the central nervous system. CDKL5 localizes both in the cytoplasm and nucleus in a brain region and development-dependent fashion (Hector et al., 2016). CDKL5 was also found to be present in excitatory postsynaptic structures, where it regulates dendritic spine maturation and growth, and controls excitatory synaptic function (Della Sala et al., 2016; Ricciardi et al., 2012). Synaptic localization of CDKL5 is mediated by its interaction with the palmitoylated form of postsynaptic density protein 95 (PSD-95) (Zhu et al., 2013; Zhang et al., 2014). Our recent investigations in CDKL5-KO mice have disclosed that CDKL5 controls the molecular organization of excitatory synapses, the turnover of dendritic spines, and the excitatory-inhibitory balance of intrinsic circuits in somatosensory and visual cortical areas as well as the establishment of parvalbumin-expressing interneurons (PV^+ INs) assembly (Della Sala et al., 2016; Pizzo et al., 2016).

Nevertheless, whilst we have started to elucidate how CDKL5 regulates the molecular composition and structure of cortical synapses, no data are yet available about the role of CDKL5 either in the organization of thalamocortical (TC) projections, which deliver incoming sensory stimuli to the cortex (Petersen, 2007), or in experience-dependent synaptic plasticity *in vivo*. This information is particularly important as an emerging view suggests that altered encoding of sensory inputs during development is not only critical for sensory-motor responses, but also underlies anxiety and atypical social behavior (Orefice et al., 2016). Notably, mounting evidences posit that autistic features may stem from impaired sensory processing (Robertson

and Baron-Cohen, 2017). The vast majority of autistic patients, including individuals affected by fragile X syndrome (FXS), a syndromic form of autism-spectrum disorder (ASD), reported abnormal sensory perception (Sinclair et al., 2015; Robertson and Baron-Cohen, 2017). Therefore, in the present study, we first aimed at addressing how CDKL5 regulates the TC connectivity in the barrel cortex (BC) of the mouse brain which relays tactile information from the whiskers to layer IV for further processing (Feldmeyer et al., 2013). Furthermore, since sensory experience shapes and optimizes neural circuits information processing by promoting structural and functional changes (Holtmaat and Svoboda, 2009), we investigated CDKL5 involvement in sensory-induced TC plasticity. Importantly, previous studies have revealed that whisker-to-BC pathway can undergo experience-induced plasticity also in adulthood (Fox et al., 2002; Feldman and Brecht 2005; Yang et al., 2009; Yu et al., 2012; Chung et al., 2017). Finally by employing a whisker specific behavioural test, we assessed that the lack of CDKL5 also impact tactile sensory responses.

EXPERIMENTAL PROCEDURES

Animals

Animal care and handling throughout the experimental procedures were conducted in accordance with European Community Council Directive 86/609/EEC for care and use of experimental animals, with protocols approved by the Italian Minister for Scientific Research (Authorization number 175/2015-PR) and the Bioethics Committee of the University of Torino. Animal suffering was minimized, as was the number of animals used. Mice for testing were obtained by crossing Cdkl5$^{-/+}$ females with Cdkl5$^{-/y}$ males and Cdkl5$^{-/+}$ females with Cdkl5$^{+/y}$ males (Amendola et al., 2014). Littermate controls were used for all the experiments. After weaning, mice were housed three to five per cage on a 12 h light/dark cycle (lights on at 7:00 h) in a temperature-controlled environment (21 ± 2° C) with food and water provided *ad libitum*. Six-week old male Cdkl5$^{-/y}$ mice and wild-type (WT) littermates were used throughout the study. Mice allocation to experimental groups was randomized by assigning random numbers to animals. Mice were included in the experimental groups only if displayed normal body weight and coat appearance indicating overall good health.

Sensory enrichment

Sensory enrichment was performed by placing the mice for two days in standard cages containing strings of plastic beads hanging from the top. The positions of bead strings were changed daily. Animals were free to navigate in the cage through the strings of beads which passively stimulated animals' whiskers. Animals housed both in the sensory enriched and standard environment were provided with food and water *ad libitum* (Yang et al., 2009).

Immunofluorescence

Animals were anesthetized with an intraperitoneal injection of Zoletil/Xylazine (Sigma-Aldrich) and transcardially perfused, first with ~ 10 ml PBS and then with ice-cold paraformaldehyde [4% in 0.1 M phosphate buffer (PB), pH 7.4]. After perfusion, the brains were then dissected and kept in the same fixative solution overnight at 4°C. Afterwards, brains were cryoprotected by immersion in 10, 20, and 30% sucrose-PB solutions, cut in 30 μm sections with a cryostat and stored at -20°C in a solution containing 30% ethylene glycol and 25% glycerol until use. For immunofluorescence processing, after several PBS rinses cryosections were kept in a solution containing 0.05% Triton X-100 and 10% normal donkey serum (NDS) in PBS for 1 h, followed by overnight incubation at 25°C with the appropriate primary antibodies (anti-c-fos, 1:500, # 2250S, Cell Signaling Technology; anti-pan-Homer,

1:500, # 160-103, Synaptic Systems; anti-VGAT, 1:500, # 131-002, Synaptic Systems; anti-VGluT1, 1:5000, # 5905, Millipore; anti-VGluT2 1:2000, # 2251, Millipore). Antibodies were diluted in PBS with 3% NDS and 0.05 Triton X-100. The following day, the sections were washed and incubated with suitable fluorescent secondary antibodies (1:1000; Jackson ImmunoResearch, West Grove, PA, USA) followed by NeuroTrace (1:500, N-21480, Molecular Probes, Eugene, USA) when appropriate. After several PBS rinses, the sections were mounted on gelatin-coated glass slides and coverslipped with Dako fluorescence mounting medium (Dako Italia, Milan, Italy).

Immunofluorescence image analysis

All analyses were carried out by an investigator who was blind to the genotype and environmental exposure. The location of the BC was identified using standard indications: 1.1 mm posterior to the Bregma and 3.4 mm lateral from the midline (Yang et al., 2009), and cortical layers were identified as in Tomassy et al. (2014). Synaptic puncta in the neuropil were analyzed in 5-10 mice per group as indicated for each experimental dataset in the results section. Stacks of 6 optical sections (0.5 μm Z-step size) were acquired from layer IV with a laser scanning confocal microscope (LSM5 Pascal; Zeiss, Germany) using a 100× objective (1.4 numerical aperture) and the pinhole set at 1 Airy unit. Synaptic puncta were quantified with the "Multi Points Measure Tool" of Imaris Software (Bitplane, Switzerland). Fluorescent puncta were considered for analysis if they were present in at least two consecutive optical sections, and dots smaller than 0.1 × 0.1 μm in the x-y axes were excluded (Luikart et al., 2005). Co-apposition between postsynaptic Homer$^+$ puncta and VGluT1$^+$ or VGluT2$^+$ axon terminals was assessed by visual inspection in the three orthogonal planes with an Imaris-dedicated tool. Puncta were considered as co-apposed ("synaptic" appositions) when no black pixels were detected between pre- and postsynaptic signals (Morello et al., 2018).

To quantify inhibitory synapses on the soma of pyramidal cells, the number of VGAT$^+$ boutons outlining the profile of identified pyramidal neurons was divided by the perimeter length measured in NeuroTrace-stained pyramidal cells using ImageJ software.

For the analysis of c-Fos$^+$ cell density, confocal images of the BC were acquired in at least 3 corresponding coronal brain sections from at least 6 animals per group with a 20× objective using a 1-μm Z-step. Digital boxes spanning from the pial surface to the corpus callosum were superimposed at matched locations on each coronal section of the BC, and divided into 10 equally sized sampling areas (bins; layer I: bin 1; layer II/III: bins 2–3; layer IV: bins 4–5; layer V: bins 6–7; layer VI: bins 8–10). Immunopositive cells were manually counted in each bin.

Whisker Nuisance Task (WNT)

Test was conducted as in McNamara et al. (2010) and Chelini et al. (2019) with few modifications. The test was performed at the end of the exposure to the either standard or enriched environment (Fig. 4A). On the five days before the test, animals were let to familiarize with handling of the experimenter and with the empty test cage (33,1 × 15,9 × 13,2 cm) (experimental cage) for one hour each day. Habituation to the novel cage was promoted by placing a small amount of the home-cage bedding overnight: bedding was removed before introducing the mouse into the experimental cage. The same 1h habituation to the test cage and experimenter was performed on the test day prior to the whisker stimulation. The test consisted in a continuous touch of the whiskers with the wooden stick (bilateral stimulation) for three consecutive sessions of 5 minutes (15 min in total) separated by a 1 min pause. The actual stimulation was preceded by a 5 min-sham stimulation where the stick was introduced in the test cage but no contact with the animal's whiskers or body occurred. During the test sessions, animals were scored according to McNamara et al. (2010) and Chelini et al. (2019) scale with few modifications. We monitored 5 different parameters: fearful behaviour, stance, evasion, response to stick and grooming, which were classified from 0 to 2 according to the response (0 = absent/typical, 1 = present/light response and 2 = profound/accentuated response). Compared to the scale published by McNamara et al. (2010) three categories were omitted: whisker position and whisking response were not evaluated as they could not be reliably scored in preliminary observations; breathing behaviour (hyperventilation) was also excluded as recent studies revealed basal respiratory abnormalities in Cdkl5 mutant mice (Lo Martire et al., 2017; Lee et al., 2018) which might affect breathing responses to whiskers stimulation.

Statistical analysis

All data are reported as mean ± SEM, with *n* indicating the number of mice. Statistical analysis was performed using Prism software (Graphpad, La Jolla, CA, USA). Puncta density, c-Fos^{+} cells density and behavioural data were analysed using 2-way analysis of variance (ANOVA) with genotype (Cdkl5$^{+/y}$, Cdkl5$^{-/y}$) and environment (SE, EE) as fixed factors and mouse as random factor followed by Fisher's LSD *post hoc* test. The analysis of the temporal progression of WN scores was performed by using 2-way ANOVA with repeated measurements (RM). Mean ± SEM and p values for each analysis are reported in Table 1. From all analyses, outliers values were excluded according to the "identify outliers" function (Method: ROUT, Q = 1%) present in Prism software (Graphpad, La Jolla, CA, USA). Power analysis of the statistical tests was performed using G_Power 3.1.9.2 (RRID:SCR_013726). The power of the statistical tests is reported in Table 2.

RESULTS

CDKL5 deficiency does not affect the number of axon terminals layer IV of the BC.

To investigate thalamic inputs to the BC, we used an antiserum against the vesicular glutamate transporter 2 (VGluT2), which labels selectively thalamic axon terminals in layer IV (Nahmani & Erisir 2005; Bopp et al., 2017). This analysis revealed no differences of $VGluT2^+$ puncta density between WT and mutant mice under non-stimulated conditions (SE) (SE-$Cdkl5^{+/y}$ vs SE-$Cdkl5^{-/y}$ $p = 0.53$; $n = 8$). Notably, two days of enriched sensory experience **(**EE) elicited a similar robust increase in the density of $VGluT2^+$ synaptic terminals in both WT and KO mice (Environment, $F_{(1,28)} = 12.26$, $p < 0.01$; SE-$Cdkl5^{+/y}$ vs EE-$Cdkl5^{+/y}$ $p < 0.05$; SE-$Cdkl5^{-/y}$ vs EE-$Cdkl5^{-/y}$ $p < 0.05$; EE-$Cdkl5^{+/y}$ vs. EE-$Cdkl5^{-/y}$ $p = 0.55$; $n = 8$) (Fig. 1A, B). Thus, these experiments indicate that the deletion of Cdkl5 does not affect experience-induced changes in the number of thalamic afferents in the BC.

Cortical neurons residing in layer IV, besides being strongly driven by thalamic inputs, receive excitatory synaptic inputs from neighbouring cortical cells (Harris and Mrsic-Flogel 2013; Schoonover et al., 2014). This local circuitry processes and integrates both horizontal and top-down sensory information within a functional column and between neighbouring barrels (Schubert et al., 2003). To investigate intracortical inputs in layer IV, we used an antibody against the vesicular glutamate transporter 1 (VGluT1), that labels selectively intracortical glutamatergic presynapses (Fremeau et al., 2014). We first quantified the overall density of $VGluT1^+$ boutons and found no differences between WT and Cdkl5 mutants under standard conditions (SE-$Cdkl5^{+/y}$ vs SE-$Cdkl5^{-/y}$ $p = 0.89$; $n = 4$-5) and after EE (EE-$Cdkl5^{+/y}$ vs EE-$Cdkl5^{-/y}$ $p = 0.18$; $n = 4$-5) (Fig. 1C, D). In contrast to what we found for thalamic afferents, EE did not produce any changes in the density of $VGluT1^+$ intracortical presynapses in both genotypes (SE-$Cdkl5^{+/y}$ vs. EE-$Cdkl5^{+/y}$ $p = 0.74$; SE-$Cdkl5^{-/y}$ vs. EE-$Cdkl5^{-/y}$ $p = 0.22$). Thus, EE increases the density of TC afferents in both WT and Cdkl5 mutant animals but does not affect intracortical presynapses.

The pre- post-synaptic configuration is atypical in Cdkl5 $^{-/y}$ mice and is restored by enriched sensory experience.

We next analysed the apposition of VGluT2 with Homer to evaluate whether thalamic afferents establish correct contacts with postsynaptic targets in layer IV of the BC. Previous studies have demonstrated that Homer is a reliable postsynaptic marker of axospinous contacts (Meyer et al., 2014) indicating that a $Homer^+$ immunopunctum faithfully identifies a dendritic spine. Surprisingly, we found that under normal conditions the density of VGluT2-Homer appositions

was significantly lower in Cdkl5-KO mice when compared to WT littermates (SE-Cdkl5$^{+/y}$ vs SE-Cdkl5$^{-/y}$ $p < 0.05$; n = 6) (Fig. 2A, B). In fact, VGluT2^{+} terminals lacking an identifiable postsynaptic partner were observed in both genotypes but were significantly more abundant in CDKL5 mutants (SE-Cdkl5$^{+/y}$ vs SE-Cdkl5$^{-/y}$ $p < 0.05$; n = 6) (Fig. 2C). Moreover, Cdkl5-KO mice exhibited a lower density of afferent terminals establishing multiple contacts with Homer^{+} spines (SE-Cdkl5$^{+/y}$ vs SE-Cdkl5$^{-/y}$ $p < 0.05$; n = 6) (Fig. 2C). These observations indicate that the formation and/or stabilization of axospinous TC synapses in layer IV is affected by deletion of Cdkl5.

We then investigated the effects of EE on TC axospinous appositions. In WT mice, EE led to an increase in the density of VGluT2^{+} terminals contacting Homer^{+} spines (SE-Cdkl5$^{+/y}$ vs EE-Cdkl5$^{+/y}$ $p < 0.05$; n = 6) (Fig. 2B). However, the percentage of terminals lacking a Homer^{+} spine as well as that of terminals contacting multiple Homer^{+} spines remained unchanged (VGluT2^{+} with 0 Homer^{+}: SE-Cdkl5$^{+/y}$ vs EE-Cdkl5$^{+/y}$ $p = 0.57$; VGluT2^{+} with 2 Homer^{+}: SE-Cdkl5$^{+/y}$ vs EE-Cdkl5$^{+/y}$ $p = 0.48$, n = 6) (Fig. 2C). These data suggest that in WT animals EE causes an overall increase in the number of thalamo-cortical synapses, without altering the configuration of axo-spinous contacts. In contrast, EE promoted a clear remodelling of TC connections in mutant mice. In fact, not only the density of VGluT2-Homer appositions increased to WT levels after EE (SE-Cdkl5$^{-/y}$ vs EE-Cdkl5$^{-/y}$ $p < 0.05$; EE-Cdkl5$^{+/y}$ vs EE-Cdkl5$^{-/y}$ $p = 0.08$, n = 6) (Fig. 2B), but this was also accompanied by a significant decrease in the percentage of terminals without a Homer^{+} spine (SE-Cdkl5$^{-/y}$ vs EE-Cdkl5$^{-/y}$ $p < 0.05$) (Fig. 2C). These data indicate that sensory stimulation triggers the remodeling of TC connections in Cdkl5$^{-/y}$ mice, restoring a synaptic configuration similar to WT condition.

Next, we examined the organization of CC connections by assessing the number of VGluT1-Homer appositions. As for the TC contacts, the organization of CC synapses was altered in Cdkl5 mutants, both under SE and after EE. Under basal conditions the density of VGluT1-Homer appositions was significantly lower in Cdkl5-KO mice when compared to WT littermates (SE-Cdkl5$^{+/y}$ vs SE-Cdkl5$^{-/y}$ $p < 0.05$; n = 5) (Fig. 2D, E). Accordingly, Cdkl5 mutants showed a higher percentage of terminals without a Homer^{+} spine (SE-Cdkl5$^{+/y}$ vs SE-Cdkl5$^{-/y}$ $p < 0.01$) as well as a lower percentage of terminals contacting two or more spines (SE-Cdkl5$^{+/y}$ vs SE-Cdkl5$^{-/y}$ $p < 0.05$) (Fig. 2F). Moreover, whereas EE did not promote any change in the density or configuration of axo-spinous synapses in WT mice (SE-Cdkl5$^{+/y}$ vs EE-Cdkl5$^{+/y}$ $p = 0.42$; n = 5) (Fig. 2E, F), whiskers stimulation produced a profound effect on synaptic organization in the mutants, normalizing both density (SE-Cdkl5$^{-/y}$ vs EE-Cdkl5$^{-/y}$ $p < 0.05$; n = 5) (Fig. 2E) and configuration (VGluT2^{+} with 0 Homer^{+}: EE-Cdkl5$^{+/y}$ vs EE-Cdkl5$^{-/y}$ $p = 0.35$; Fig. 2F) of VGluT1^{+}-Homer^{+} axo-spinous synapses.

Altogether, these data indicate that sensory stimulation promotes plasticity of both TC and CC synapses in layer IV of Cdkl5 mutants, restoring a connectivity configuration similar to control levels.

Lack of CDKL5 does not affect the number of inhibitory synapses in layer IV of the BC.

Manipulation of whisker activity was reported to lead to functional rearrangements of inhibitory circuits in layer IV of the BC, including modifications in the number of GABAergic synapses targeting excitatory neurons (Jiao et al., 2006; Knott et al., 2002) as well as in the intrinsic properties of interneurons (Sun, 2009). Despite these previous observations, we estimated that the density of GABAergic synapses targeting the cell body of pyramidal neurons was similar in Cdkl5-KO and WT mice and was not influenced by EE (Genotype, $F_{(1,17)} = 12.26$, $p = 0.86$; environmental exposure, $p = 0.43$; genotype x environmental exposure, $p = 0.47$; $n = 5$) (Fig. 3A, B). Moreover, there were no differences in the density of inhibitory synapses between WT and KO mice also in the neuropil of layer IV both under SE (SE-Cdkl5$^{+/y}$ vs SE-Cdkl5$^{-/y}$ $p = 0.70$; $n = 5$) (Fig. 3C, D) and after EE (SE-Cdkl5$^{+/y}$ vs EE-Cdkl5$^{+/y}$ $p = 0.77$; SE-Cdkl5$^{-/y}$ vs EE-Cdkl5$^{-/y}$ $p = 0.87$; EE-Cdkl5$^{+/y}$ vs EE-Cdkl5$^{-/y}$ $p = 0.63$; $n = 5$). Thus, these data show that deletion of CDKL5 does not induce major basal or activity-dependent structural rearrangements of GABAergic circuitry in layer IV of BC.

Cdkl5-KO mice show abnormal behavioural responses to whisker stimulation.

To investigate the functional impact of the synaptic defects revealed in the BC of Cdkl5-KO mice, we probed mice with a behavioural paradigm, the WNT (McNamara et al., 2010; Learoyd et al., 2012; Fontes-Dutra et al 2018; Chelini et al, 2019), designed to test whisker-related somatosensory responses in mice. During the three 5-min sessions of whisker stimulation, 5 different behaviours were scored (see Materials and Methods). In the SE exposed animals no differences between genotypes were detected during the sham session, when the wooden stick was presented in close proximity of the animal's head without any tactile contact (SE-Cdkl5$^{+/y}$ vs SE-Cdkl5$^{-/y}$ $p = 0.21$; $n = 9$). Moreover, no differences in the total WN scores were found between WT and mutant mice (SE-Cdkl5$^{+/y}$ vs SE-Cdkl5$^{-/y}$ $p = 0.21$; $n = 9$) (Fig. 4B). Intriguingly, when analyzed the temporal progression of the scores across trials, we found that KO mice exhibited statistically significant lower scores only in the first trial (SE-Cdkl5$^{+/y}$ vs SE-Cdkl5$^{-/y}$ $p < 0.01$; $n = 9$) (Fig. 4D), whilst no difference was not detected in trials 2 and 3 (Trial 2: SE-Cdkl5$^{+/y}$ vs SE-Cdkl5$^{-/y}$ $p = 0.60$; Trial 3: SE-Cdkl5$^{+/y}$ vs SE-Cdkl5$^{-/y}$ $p = 0.63$; $n = 9$). This was due to a significant reduction of the overall responses shown by the WT mice across trials (SE-Cdkl5$^{+/y}$, Trial 1 vs Trial 3, $p < 0.05$; $n = 9$), whereas in Cdkl5 mutants WN

scores were unchanged (SE-Cdkl5$^{-/y}$, Trial 1 vs Trial 3, p = 0.07; n = 9). The exposure to EE did not produce changes in the overall WN score both in WT (SE-Cdkl5$^{+/y}$ vs EE-Cdkl5$^{+/y}$ p = 0.18; n = 9) and mutant mice (SE-Cdkl5$^{-/y}$ vs EE-Cdkl5$^{-/y}$ p = 0.32; n = 9) (Fig. 4B), a trend that was maintained in the analysis across trials (SE-Cdkl5$^{+/y}$ vs EE-Cdkl5$^{+/y}$, Trail 1 p = 0.96; Trail 2 p = 0.25; Trail 3 p = 0.08; SE-Cdkl5$^{-/y}$ vs EE-Cdkl5$^{-/y}$ Trail 1: p = 0.89; Trail 2 p = 0.51; Trail 3 p = 0.11; n = 9) (Fig. 4C). However, the reduction of responses from the first to the third trial shown by SE WT was not detected in EE WT mice (EE-Cdkl5$^{+/y}$, Trial 1 vs Trial 3, p = 0.86; n = 9) (Fig. 4E). Interestingly, the EE-KO mice exhibited an inter-trial increase of the responses (EE-Cdkl5$^{-/y}$: Trial 1 vs Trial 3 $p < 0.05$; n = 9) (Fig. 4F). Finally, we individually analyzed the responses for the five parameters used to calculate the overall WN score. Interestingly, we found that under basal conditions Cdkl5 mutant mice displayed reduced values for both freezing behaviour (SE-Cdkl5$^{+/y}$ vs SE-Cdkl5$^{-/y}$ $p < 0.05$; n = 9) (Fig. 4H) and stance (SE-Cdkl5$^{+/y}$ vs SE-Cdkl5$^{-/y}$ $p < 0.001$) (Fig. 4I), while scores for both stick responses (SE-Cdkl5$^{+/y}$ vs SE-Cdkl5$^{-/y}$ $p < 0.01$) (Fig. 4J) and grooming were increased (SE-Cdkl5$^{+/y}$ vs SE-Cdkl5$^{-/y}$ $p < 0.05$) (Fig. 4L) compared to WT animals. No differences were detected for evasion scores (SE-Cdkl5$^{+/y}$ vs SE-Cdkl5$^{-/y}$ p = 0.29) (Fig. 4K). EE did not induce major changes in the WT mice (freezing: SE-Cdkl5$^{+/y}$ vs EE-Cdkl5$^{+/y}$ p = 0.09; stance: SE-Cdkl5$^{+/y}$ vs EE-Cdkl5$^{+/y}$ p = 0.39; stick response: SE-Cdkl5$^{+/y}$ vs EE-Cdkl5$^{+/y}$ p = 0.48; grooming: SE-Cdkl5$^{+/y}$ vs EE-Cdkl5$^{+/y}$ p = 0.13; n = 9) (Fig. 4H-L) beside a reduction in the evasion levels (evasion: SE-Cdkl5$^{+/y}$ vs EE-Cdkl5$^{+/y}$ $p < 0.05$). On the other hand, EE led to robust changes in the KO animals behaviours: indeed, EE suppressed almost all behavioural abnormalities shown by SE mutants, except grooming (freezing: SE-Cdkl5$^{-/y}$ vs EE-Cdkl5$^{-/y}$ $p < 0.01$; stance: SE-Cdkl5$^{-/y}$ vs EE-Cdkl5$^{-/y}$ $p < 0.01$; stick response: SE-Cdkl5$^{-/y}$ vs EE-Cdkl5$^{-/y}$ $p < 0.05$; grooming: SE-Cdkl5$^{-/y}$ vs EE-Cdkl5$^{-/y}$ p = 0.16; n = 9) (Fig. 4H-L).

The activation of c-Fos is reduced in the BC of Cdkl5-KO mice following whisker stimulation.

It has been previously reported that whisker tactile stimulation can produce an increase of c-Fos expression, an established marker of neuronal activity, in the BC (Filipkowski et al., 2000; Lecrux et al., 2017; Chelini et al., 2019). To assess tactile-induced neuronal activity in the BC, we investigated the levels of expression of c-Fos 2 hours after the end of WNT administration. Two-way analysis revealed a significant Genotype x Environment effect (two-way ANOVA, Genotype x Environment, $F_{(1,22)} = 9.47$, $p < 0.01$; Genotype, $F_{(1,22)} = 0.84$, p = 0.37; Environment, $F_{(1,22)} = 0.01$, p = 0.91; n = 6-8). Fisher's LSD post-hoc test showed a reduced

expression of c-Fos in BC layer IV of Cdkl5-KO mice compared to WT animals under SE (SE-Cdkl5$^{+/y}$ vs SE-Cdkl5$^{-/y}$ $p < 0.05$; n = 6) (Fig. 5A, B), indicating that loss of CDKL5 produces an impairment in stimuli-induced neuronal activation. Importantly, exposing mutants to EE increased c-Fos immunoreactivity in the BC (layer IV: SE-Cdkl5$^{-/y}$ vs EE-Cdkl5$^{-/y}$ $p < 0.001$; n = 6-8), to levels similar to SE-WT mice. Conversely, EE-WT mice showed a robust reduction in c-Fos^{+} cells in layers II-III compared to SE animals (SE-Cdkl5$^{+/y}$ vs EE-Cdkl5$^{+/y}$ $p < 0.05$; n = 6) and IV (SE-Cdkl5$^{+/y}$ vs EE-Cdkl5$^{+/y}$ $p < 0.01$; n = 6).

Overall, the present data suggests that the defective connectivity due to CDKL5 loss might underlie an abnormal cortical delivery and processing of tactile stimuli and, importantly, that enhancement of sensory experience might have, to some extent, beneficial effects on both cortical circuitry organization and responsiveness.

DISCUSSION

In this study, we investigated the synaptic organization of BC circuits underlying tactile sensory processing in a mouse model of CDD where we analysed structural and behavioural plasticity produced by prolonged sensory stimulation. Our investigation has several major findings.

First, the absence of CDKL5 leads to altered numerosity and configuration of both TC and CC synapses as illustrated by a higher percentage of solitary presynaptic terminals, even though the number of both thalamic afferents targeting layer IV neurons and CC excitatory terminals was preserved. Second, these synaptic abnormalities were associated with both reduced neuronal activation and altered whisker-stimulation mediated behavioural responses. Third, we demonstrated that a two-day long sensory stimulation promoted structural synaptic plasticity in both WT and mutant mice, restoring in Cdkl5-KOs the density and configuration of $VGluT2^+$ and $VGluT1^+$ axospinous synapses, neuronal activation and whisker-stimulation related behavioural responses.

The normal density of $VGluT2^+$ and $VGluT1^+$ terminals in cortical layer IV that we report in adult mutant mice suggests that CDKL5 deficiency has no detrimental impact on the ability of thalamic and cortical afferents to reach their targets. Rather, the reduced density of axo-spinous contacts in layer IV points out that CDKL5 may be involved in the stabilization phase of excitatory synapses by regulating the postsynaptic molecular mechanisms responsible for spine maturation and trans-synaptic stabilization. Accordingly, previously published data indicate that, in the somatosensory cortex of Cdkl5-KO mice, dendritic spines show reduced spine-head size together with abnormally increased turnover (Della Sala et al., 2016), pointing to a reduced ability of forming stable synapses. There are several molecular mechanisms that can explain how loss of CDKL5 produces these synaptic alterations. One of the first identified CDKL5 interactors is PSD-95 (Zhu et al., 2013), a postsynaptic scaffolding protein that stabilizes newly-formed synaptic contacts (Taft and Turrigiano, 2014) by regulating molecular interactions at both the postsynaptic (Béïque et al., 2006; Chen et al., 2011; Ehrlich et al., 2007; El-Husseini et al., 2000) and presynaptic compartment (Futai et al., 2007; Hruska et al., 2015). Deletion of CDKL5 was reported to reduce the synaptic expression of PSD-95 in the neocortex (Della Sala et al., 2016: Pizzo et al., 2016) and to prevent the phosphorylation of the synaptic adhesion molecule NGL-1, thus leading to defects in synapse maturation and stabilization (Ricciardi et al., 2012). Accordingly, the reduced connectivity with $Homer^+$ structures, which represent structurally and functionally mature spines, in the BC of Cdkl5 mutants further supports a primary role of CDKL5 in the anatomical and functional integrity of dendritic spines and is

suggestive of an excessive number of immature and/or silent - i.e.: with impaired neurotransmission capabilities - synaptic contacts.

Recent findings indicate that CDKL5 may regulate dendritic spines not only by interacting with PDS-95 but also by directly binding with microtubule-associated proteins such as the IQ Motif Containing GTPase Activating Protein 1 (IQGAP1) (Barbiero et al., 2017) and MAP1S, EB2 and ARHGEF2 (Baltussen et al., 2018). Furthermore, CDKL5 might regulate dendritic spines composition and function by controlling the transcriptional levels of key components of dendritic spines. Indeed, Trazzi et al. (2016) reported that CDKL5 phosphorylates HDAC4 thus preventing HDAC4 translocation into the nucleus and promoting the expression of genes essential for synaptic transmission and information processing such as CamKIIα and SNAP25 (Sando III et al., 2012).

Our anatomical findings suggest that the delivery of sensory inputs to the cortex might be less efficient in Cdkl5 mutants. Indeed, WNT-induced cortical activation was profoundly reduced in Cdkl5 KO mice as well as their behavioural responses to whisker stimulation. Reduced cortical responsiveness to visual and auditory stimuli were previously reported in Cdkl5 mutants (Mazziotti et al., 2017; Wang et al., 2012). Remarkably, several animal models of ASD, such as fragile X mental retardation protein 1 (Fmr1), Engrailed-2 (En2), and (Mecp2) mutant mice, exhibit abnormal sensitivity to somatosensory stimuli (Chelini et al., 2018; He et al., 2017; Orefice et al., 2016; Zhang et al., 2014), together with functional connectivity defects in sensory brain areas (Chelini et al., 2018; Haberl et al., 2015; Lee et al., 2017; Zerbi et al., 2018). The analysis of WNT parameters further revealed that the altered scores obtained by Cdkl5 KO mice were mainly due to lower values for freezing and stance, suggestive of reduced fear. This idea is supported by the deficits in a fear-conditioning paradigm shown by Cdkl5 null mice (Vigli et al., 2018, Wang et al., 2012). As a recent study on a mouse model of ASD revealed that impaired BC connectivity is paralleled by disruption of tactile stimuli processing, amygdala activation and fear behaviour (Chelini et al., 2019), we hypothesise that similar abnormalities may underlie fear reduction in Cdkl5 KO mice. In contrast, Cdkl5 mutants exhibited higher scores for stick response and grooming. Many evidences have pointed out that increased grooming activity may reflect an atypical activation of the striatum (Kalueff et al., 2016) which integrates sensory inputs, including tactile stimuli, processed in the BC (Reig and Silberberg, 2014). Given that the striatum and the neocortex are directly and indirectly interconnected in movement-control networks, it is tempting to speculate that increased grooming shown by CDKL5 mutants is produced by altered activity of the striatum or of other brain regions functionally connected with the BC. Moreover, the analysis of the temporal progression of WNT scores revealed, in agreement with a previous study (Chelini et al., 2019), that WT mice

exhibited a reduction in the WNT scores across trials, indicating that mice tend to habituate to repeated whisker stimulations. In contrast, mutants did not show any habituation suggesting that Cdkl5 is important for adaptation processes. A similar atypical habituation to whisker stimulation was shown by Fmrp KO mice (He et al., 2017), suggesting that sensory impairments associated with both FXS and CDD may stem from common mechanisms. One possibility is that atypical habituation shown by Cdkl5 mutants originates from abnormal sensorimotor gating in response to tactile inputs. This hypothesis is supported by deficits in prepulse inhibition (PPI) of startle reflex in response to acoustic stimuli displayed by Cdkl5-null mice (Vigli et al., 2018). Intriguingly, atypical sensorimotor gating in a tactile prepulse inhibition test was revealed also in other models of ASD such as Mecp2, Fmr1 and Gabrb3 mutants, further supporting the concept that impairments in mechanisms underlying cortical processing of sensory information may contribute to ASD disorders (Orefice et al., 2016; Zhang et al., 2014).

Besides impairments affecting glutamatergic connectivity, atypical processing and integration of sensory inputs in Cdkl5-KO mice can derive from changes in the GABAergic system (Griffen and Maffei, 2014). However, in our settings, no apparent defects were detected in GABAergic circuits in Cdkl5-KO and WT. This is somehow surprising given our previous evidences in primary visual cortex, where deficiency of CDKL5 caused an increased density of $VGAT^{+}$ puncta, including those establishing perisomatic synapses (Pizzo et al., 2016). One possible explanation for these discrepancies is that the impact of Cdkl5 deficiency on GABAergic circuitry is layer and region specific. A similar region-specific alteration of GABAergic circuitry has been reported in Mecp2-KO mice. In this mouse model, a robust enhancement of GABAergic transmission and connectivity was observed in S1 (Dani et al., 2005) and V1 (Durand et al., 2012), leading to a shift in the balance between excitation and inhibition in favour of the latter and to reduced cortical activity; on the other hand, no effects of MeCP2 deletion on inhibitory synaptic currents were found in the medial prefrontal cortex (Sceniak et al., 2016). Therefore CDKL5, like Mecp2, may differentially regulate the organization of GABAergic systems, leading to different functional outcomes in distinct neural circuits.

TC projections are very plastic in adulthood and can undergo extensive experience-dependent rewiring (Oberlaender et al., 2012; Yu et al., 2012). For instance, prolonged whiskers stimulation was proven to increase axospinous synapses in BC layer IV (Knott et al., 2002), whereas whiskers trimming induced a reduction in the overall density of TC synapses in adult rat barrel cortex (Wimmer et al., 2010; Oberlaender et al., 2012). In agreement with these observations, we found that EE produced in WT mice an increase in the density of TC synapses.

In contrast, we did not detect any changes in CC glutamatergic synapses in EE WT animals. Notably, manipulations of sensory inputs may modify the strength of excitatory connections by adjusting the size of axonal inputs, dendritic spines and interposed contact zones, without affecting synapse number (Cheetham et al., 2007; 2014). Interestingly, the EE-induced increase of TC connections was paralleled by a striking reduction in cortical activity as revealed by the c-Fos staining. We speculate that this effect may arise from sensory adaptation mechanisms (Whitmire and Stanley, 2016). Indeed, prolonged whisker stimulation was shown to decrease neuronal responsivity of layer IV neurons to whisker deflection (Chung et al., 2002; Knott et al., 2002; Khatri et al., 2004; Katz et al., 2006; Quairiaux et al., 2007). Neuronal adaptation to repeated sensory stimulation occurs across all sensory modalities and governs crucial processes such as stimulus detection and discriminability (Castro-Alamancos, 2004; Ollerenshaw et al., 2014). Notably, EE did not promote major changes in WNT-related behaviours indicating no EE-mediated alterations in tactile stimuli processing. However, in contrast to SE-WT animals, no behavioural habituation during WNT was found in the EE-WT mice. We suspect that the increased tactile stimuli experienced during the 2-day long exposure to an enriched environment promoted behavioural habituation to whisker-mediated sensory inputs, thus reducing the adaptation extent potentially elicited by WNT. The decrease in the evasion scores, suggestive of reduced flight responses, supports this notion.

Importantly, we showed that stimulation-induced synaptic plasticity was retained in Cdkl5 mutant mice, even though it was qualitatively different from that occurring in WT mice. Indeed, EE was able to induce not only an increase in the number and a reorganization of TC synapses but also an additional restructuring of intracortical connectivity, leading to a restoration of CC connections to WT levels. Furthermore, exposure to EE re-established neuronal activity levels in BC of mutants. These pieces of evidence are particularly important as they suggest that sensory stimulation might elicit a more general reorganization of circuitry in the mutants, possibly leading to the alleviation of phenotypic abnormalities. Indeed, EE exposure caused a correction in most of the behavioural WTN parameters which were altered in Cdkl5-KO mice. Accordingly, the enhancement of sensory experience was proven to be beneficial for both the synaptic and behavioural deficits affecting mouse models of pervasive neurodevelopmental disorders, such as Mecp2 and FMR1 KO mice (Kerr et al., 2010; Kondo et al., 2008; Lonetti et al., 2010; Restivo et al., 2005).

Overall, our present findings disclose for the first time a primary role of CDKL5 in mechanisms involved in the formation and maintenance of cortical circuitry underlying tactile sensory information processing. Together with our behavioural analyses, showing atypical whisker-mediated responses, these data suggest that sensory defects may underlie the appearance of

ASD traits in CDD. Moreover, our data posit that affected cortical circuits can effectively undergo structural remodelling: importantly, the re-establishment of correct cortical circuitry by sensory enhancement, paralleled by improvements in behavioural responses to sensory stimuli, strongly supports the use of enhanced sensory stimulation as a therapeutic strategy for CCD patients.

ACKNOWLEDGEMENTS

The authors are grateful to Dr. Francesco Libera and Prof. Yuri Bozzi for precious technical assistance and fruitful advices. The work was funded by L'Albero di Greta [Albero di Greta-Giustetto2018], Fondazione Telethon [GGP15098B], International Foundation for CDKL5 Research [IFCR-Giustetto2019] and Association Française du Syndrome de Rett [ASFR-Giustetto 2017].

REFERENCES

Amendola E, Zhan Y, Mattucci C, Castroflorio E, Calcagno E, Fuchs C, Lonetti G, Silingardi D, Vyssotski AL, Farley D, Ciani E, Pizzorusso T, Giustetto M, Gross CT (2014) Mapping pathological phenotypes in a mouse model of CDKL5 disorder. PLoS One 9 (5): e91613.

Bahi-Buisson N, Bienvenu T (2012) CDKL5-related disorders: from clinical description to molecular genetics. Mol Syndromol. 2 (3-5): 137-152.

Baltussen LL, Negraes PD, Silvestre M, Claxton S, Moeskops M, Christodoulou E, Flynn HR, Snijders AP, Muotri AR, Ultanir SK (2018) Chemical genetic identification of CDKL5 substrates reveals its role in neuronal microtubule dynamics. EMBO J. 37 (24). pii: e99763.

Barbiero I, Peroni D, Tramarin M, Chandola C, Rusconi L, Landsberger N, Kilstrup-Nielsen C (2017) The neurosteroid pregnenolone reverts microtubule derangement induced by the loss of a functional CDKL5-IQGAP1 complex. Hum Mol Genet. 26 (18): 3520-3530.

Béïque JC, Lin DT, Kang MG, Aizawa H, Takamiya K, Huganir RL (2006) Synapse-specific regulation of AMPA receptor function by PSD-95. Proc Natl Acad Sci U S A. 103 (51): 19535-40.

Bopp R, Holler-Rickauer S, Martin KA, Schuhknecht GF (2017) An ultrastructural study of the thalamic input to layer 4 of primary motor and primary somatosensory cortex in the mouse. J Neurosci. 37 (9): 2435-2448.

Castro-Alamancos MA (2004) Dynamics of sensory thalamocortical synaptic networks during information processing states. Prog Neurobiol. 74 (4): 213-47.

Cheetham CE, Barnes SJ, Albieri G, Knott GW, Finnerty GT (2014) Pansynaptic enlargement at adult cortical connections strengthened by experience. Cereb Cortex. 24 (2): 521-31.

Cheetham CE, Hammond MS, Edwards CE, Finnerty GT (2007) Sensory experience alters cortical connectivity and synaptic function site specifically. J Neurosci. 27 (13): 3456-65.

Chelini G, Zerbi V, Cimino L, Grigoli A, Markicevic M, Libera F, Robbiati S, Gadler M, Bronzoni S, Miorelli S, Galbusera A, Gozzi A, Casarosa S, Provenzano G, Bozzi Y (2019) Aberrant somatosensory processing and connectivity in mice lacking Engrailed-2. J Neurosci. 39 (8): 1525-1538

Chen X, Nelson CD, Li X, Winters CA, Azzam R, Sousa AA, Leapman RD, Gainer H, Sheng M, Reese TS (2011) PSD-95 is required to sustain the molecular organization of the postsynaptic density. J Neurosci. 31 (17): 6329-38.

Chung S, Jeong JH, Ko S, Yu X, Kim Y2, Isaac JT4, Koretsky AP (2017) Peripheral sensory deprivation restores critical-period-like plasticity to adult somatosensory thalamocortical inputs. Cell Rep. 19 (13): 2707-2717.

Chung S, Li X, Nelson SB (2002) Short-term depression at thalamocortical synapses contributes to rapid adaptation of cortical sensory responses in vivo. Neuron. 34 (3): 437-46.

Dani VS, Chang Q, Maffei A, Turrigiano GG, Jaenisch R, Nelson SB (2005) Reduced cortical activity due to a shift in the balance between excitation and inhibition in a mouse model of Rett syndrome. Proc Natl Acad Sci U S A. 102 (35): 12560-5.

Della Sala G, Putignano E, Chelini G, Melani R, Calcagno E, Ratto GM, Amendola E, Gross CT, Giustetto M, Pizzorusso T (2016) Dendritic spine instability in a mouse model of CDKL5 disorder is rescued by insulin-like growth factor 1. Biol Psychiatry 80 (4): 302-11.

Durand S, Patrizi A, Quast KB, Hachigian L, Pavlyuk R, Saxena A, Carninci P, Hensch TK, Fagiolini M (2012) NMDA receptor regulation prevents regression of visual cortical function in the absence of Mecp2. Neuron 76 (6): 1078-90.

Ehrlich I, Klein M, Rumpel S, Malinow R (2007) PSD-95 is required for activity-driven synapse stabilization. Proc Natl Acad Sci U S A. 104 (10): 4176-81.

El-Husseini AE, Schnell E, Chetkovich DM, Nicoll RA, Bredt DS (2000) PSD-95 involvement in maturation of excitatory synapses. Science 290 (5495): 1364-8.

Feldman DE, Brecht M (2015) Map plasticity in somatosensory cortex. Science 310 (5749): 810-5.

Feldmeyer D, Brecht M, Helmchen F, Petersen CC, Poulet JF, Staiger JF, Luhmann HJ, Schwarz C (2013) Barrel cortex function. Prog Neurobiol. 103: 3-27.

Filipkowski RK, Rydz M, Berdel B, Morys J, Kaczmarek L (2000) Tactile experience induces c-fos expression in rat barrel cortex. Learn Mem. 7 (2): 116-22.

571 Fontes-Dutra M, Santos-Terra J, Deckmann I, Brum Schwingel G, Della-Flora Nunes G,
572 Hirsch MM, Bauer-Negrini G, Riesgo RS, Bambini-Júnior V, Hedin-Pereira C, Gottfried C
573 (2018) Resveratrol prevents cellular and behavioral sensory alterations in the animal model of
574 autism induced by valproic acid. Front Synaptic Neurosci. 10:9.

575 Fox K (2002) Anatomical pathways and molecular mechanisms for plasticity in the barrel
576 cortex. Neuroscience 111 (4): 799-814.

577 Fremeau RT Jr, Kam K, Qureshi T, Johnson J, Copenhagen DR, Storm-Mathisen J, Chaudhry
578 FA, Nicoll RA, Edwards RH (2004) Vesicular glutamate transporters 1 and 2 target to
579 functionally distinct synaptic release sites. Science 304 (5678): 1815-9.

580 Futai K, Kim MJ, Hashikawa T, Scheiffele P, Sheng M, Hayashi Y (2007) Retrograde
581 modulation of presynaptic release probability through signaling mediated by PSD-95-
582 neuroligin. Nat Neurosci. 10 (2): 186-95.

583 Griffen TC, Maffei A (2014) GABAergic synapses: their plasticity and role in sensory cortex.
584 Front Cell Neurosci. 8:91.

585 Haberl MG, Zerbi V, Veltien A, Ginger M, Heerschap A, Frick A (2015) Structural-functional
586 connectivity deficits of neocortical circuits in the Fmr1-/y mouse model of autism. Sci Adv. 1
587 (10): e1500775.

588 Harris KD, Mrsic-Flogel TD (2013) Cortical connectivity and sensory coding. Nature 503
589 (7474): 51-8.

590 Hector RD, Dando O, Landsberger N, Kilstrup-Nielsen C, Kind PC, Bailey ME, Cobb SR
591 (2016) Characterisation of CDKL5 transcript isoforms in human and mouse. PLoS One. 11 (6):
592 e0157758.

593 He CX, Cantu DA, Mantri SS, Zeiger WA, Goel A, Portera-Cailliau C (2017) Tactile
594 defensiveness and impaired adaptation of neuronal activity in the Fmr1 knock-out mouse model
595 of autism. J Neurosci. 37 (27): 6475-6487.

596 Holtmaat A and Svoboda K (2009) Experience-dependent structural synaptic plasticity in the
597 mammalian brain. Nat Rev Neurosci. 10 (9): 647-58.

598 Hruska M, Henderson NT, Xia NL, Le Marchand SJ, Dalva MB (2015) Anchoring and

599 synaptic stability of PSD-95 is driven by ephrin-B3. Nat Neurosci. 18 (11): 1594-605.

600 Kalueff AV, Stewart AM, Song C, Berridge KC, Graybiel AM, Fentress JC (2016)
601 Neurobiology of rodent self-grooming and its value for translational neuroscience. Nat Rev
602 Neurosci. 17 (1): 45-59.

603 Katz Y, Heiss JE, Lampl I (2006) Cross-whisker adaptation of neurons in the rat barrel cortex.
604 J Neurosci. 26 (51): 13363-72.

605 Kerr B, Silva PA, Walz K, Young JI (2010) Unconventional transcriptional response to
606 environmental enrichment in a mouse model of Rett syndrome. PLoS One 5 (7): e11534.

607 Khatri V, Hartings JA, Simons DJ (2004) Adaptation in thalamic barreloid and cortical barrel
608 neurons to periodic whisker deflections varying in frequency and velocity. J Neurophysiol. 92
609 (6): 3244-54.

610 Knott GW, Quairiaux C, Genoud C, Welker E (2002) Formation of dendritic spines with
611 GABAergic synapses induced by whisker stimulation in adult mice. Neuron 34 (2): 265-73.

612 Kondo M, Gray LJ, Pelka GJ, Christodoulou J, Tam PP, Hannan AJ (2008) Environmental
613 enrichment ameliorates a motor coordination deficit in a mouse model of Rett syndrome--
614 Mecp2 gene dosage effects and BDNF expression. Eur J Neurosci. 27 (12): 3342-50.

615 Jhang CL, Huang TN, Hsueh YP, Liao W (2017) Mice lacking cyclin-dependent kinase-like
616 5 manifest autistic and ADHD-like behaviors. Hum Mol Genet. 26 (20): 3922-3934.

617 Jiao Y, Zhang C, Yanagawa Y, Sun QQ (2006) Major effects of sensory experiences on the
618 neocortical inhibitory circuits. J Neurosci. 26 (34): 8691-701.

619 Learoyd AE, Lifshitz J (2012) Comparison of rat sensory behavioral tasks to detect
620 somatosensory morbidity after diffuse brain-injury. Behav Brain Res 226:197-204.

621 Lecrux C, Sandoe CH, Neupane S, Kropf P, Toussay X, Tong XK, Lacalle-Aurioles M,
622 Shmuel A, Hamel E (2017) Impact of altered cholinergic tones on the neurovascular coupling
623 response to whisker stimulation. J Neurosci. 37 (6): 1518-1531.

624 Lee LJ, Tsytsarev V, Erzurumlu RS (2017) Structural and functional differences in the barrel
625 cortex of Mecp2 null mice. J Comp Neurol. 525 (18): 3951-3961.

Lee KZ, Liao W (2018) Loss of CDKL5 disrupts respiratory function in mice. Respir Physiol Neurobiol. 248: 48-54.

Lo Martire V, Alvente S, Bastianini S, Berteotti C, Silvani A, Valli A, Viggiano R, Ciani E, Zoccoli G (2017) CDKL5 deficiency entails sleep apneas in mice. J. Sleep Res. 26, 495-497.

Lonetti G, Angelucci A, Morando L, Boggio EM, Giustetto M, Pizzorusso T (2010) Early environmental enrichment moderates the behavioral and synaptic phenotype of MeCP2 null mice. Biol Psychiatry 67 (7): 657-65.

Luikart BW, Nef S, Virmani T, Lush ME, Liu Y, Kavalali ET, Parada LF (2005) TrkB has a cell-autonomous role in the establishment of hippocampal Schaffer collateral synapses. J Neurosci. 25 (15): 3774-86.

Mazziotti R, Lupori L, Sagona G, Gennaro M, Della Sala G, Putignano E, Pizzorusso T (2017) Searching for biomarkers of CDKL5 disorder: early-onset visual impairment in CDKL5 mutant mice. Hum Mol Genet. 26 (12): 2290-2298.

McNamara KC, Lisembee AM, Lifshitz J (2010) The whisker nuisance task identifies a late-onset, persistent sensory sensitivity in diffuse brain- injured rats. J Neurotrauma 27: 695-706.

Meyer D, Bonhoeffer T, Scheuss V (2014) Balance and stability of synaptic structures during synaptic plasticity. Neuron 82 (2): 430-43.

Morello N, Schina R, Pilotto F, Phillips M, Melani R, Plicato O, Pizzorusso T, Pozzo-Miller L, Giustetto M (2018) Loss of Mecp2 causes atypical synaptic and molecular plasticity of parvalbumin-expressing interneurons reflecting Rett Syndrome-like sensorimotor defects. eNeuro. 5 (5). pii: ENEURO.0086-18.2018.

Nahmani M, Erisir A (2005) VGluT2 immunochemistry identifies thalamocortical terminals in layer 4 of adult and developing visual cortex. J Comp Neurol. 484 (4): 458-73.

Oberlaender M, Ramirez A, Bruno RM (2012) Sensory experience restructures thalamocortical axons during adulthood. Neuron. 74 (4): 648-55.

Ollerenshaw DR, Zheng HJV, Millard DC, Wang Q, Stanley GB (2014) The adaptive trade-off between detection and discrimination in cortical representations and behavior. Neuron. 81 (5): 1152-1164.

Orefice LL, Zimmerman AL, Chirila AM, Sleboda SJ, Head JP, Ginty DD (2016) Peripheral mechanosensory neuron dysfunction underlies tactile and behavioral deficits in mouse models of ASDs. Cell 166 (2): 299-313.

Petersen CC (2007) The functional organization of the barrel cortex. Neuron. 56 (2): 339-55.

Pizzo R, Gurgone A, Castroflorio E, Amendola E, Gross C, Sassoè-Pognetto M, Giustetto M (2016) Lack of CDKL5 disrupts the organization of excitatory and inhibitory synapses and parvalbumin interneurons in the primary visual cortex. Front Cell Neurosci. 10:261.

Quairiaux C, Armstrong-James M, Welker E (2007) Modified sensory processing in the barrel cortex of the adult mouse after chronic whisker stimulation. J Neurophysiol. 97 (3): 2130-47.

Reig R, Silberberg G (2014) Multisensory integration in the mouse striatum. Neuron. 83 (5): 1200-12.

Restivo L, Ferrari F, Passino E, Sgobio C, Bock J, Oostra BA, Bagni C, Ammassari-Teule M (2005) Enriched environment promotes behavioral and morphological recovery in a mouse model for the fragile X syndrome. Proc Natl Acad Sci U S A. 102 (32): 11557-62.

Ricciardi S, Ungaro F, Hambrock M, Rademacher N, Stefanelli G, Brambilla D, Sessa A, Magagnotti C, Bachi A, Giarda E, Verpelli C, Kilstrup-Nielsen C, Sala C, Kalscheuer VM, Broccoli V (2012) CDKL5 ensures excitatory synapse stability by reinforcing NGL-1-PSD95 interaction in the postsynaptic compartment and is impaired in patient iPSC-derived neurons. Nat Cell Biol. 14 (9): 911-23.

Robertson CE and Baron-Cohen S (2017) Sensory perception in autism. Nat Rev Neurosci. 18 (11): 671-684.

Sando R 3rd, Gounko N, Pieraut S, Liao L, Yates J 3rd, Maximov A (2012) HDAC4 governs a transcriptional program essential for synaptic plasticity and memory. Cell. 151 (4): 821-834.

Sceniak MP, Lang M, Enomoto AC, James Howell C, Hermes DJ, Katz DM (2016) Mechanisms of functional hypoconnectivity in the medial prefrontal cortex of Mecp2 null mice. Cereb Cortex. 26 (5): 1938-56.

Schubert D, Kötter R, Zilles K, Luhmann HJ, Staiger JF (2003) Cell type-specific circuits of cortical layer IV spiny neurons. J. Neurosci. 23 (7): 2961-70.

682 Schoonover CE, Tapia JC, Schilling VC, Wimmer V, Blazeski R, Zhang W, Mason CA,
683 Bruno RM (2014) Comparative strength and dendritic organization of thalamocortical and
684 corticocortical synapses onto excitatory layer 4 neurons. J Neurosci. 34 (20): 6746-58.

685 Sinclair D, Oranje B, Razak KA, Siegel SJ, Schmid S (2017) Sensory processing in autism
686 spectrum disorders and Fragile X syndrome-From the clinic to animal models. Neurosci
687 Biobehav Rev. 76 (Pt B): 235-253.

688 Sun QQ (2009) Experience-dependent intrinsic plasticity in interneurons of barrel cortex layer
689 IV. J Neurophysiol. 102 (5): 2955-73.

690 Taft CE, Turrigiano GG (2013) PSD-95 promotes the stabilization of young synaptic contacts.
691 Philos Trans R Soc Lond B Biol Sci. 369 (1633): 20130134.

692 Tomassy GS, Morello N, Calcagno E, Giustetto M (2014) Developmental abnormalities of
693 cortical interneurons precede symptoms onset in a mouse model of Rett syndrome. Neurochem.
694 131 (1): 115-27.

695 Trazzi S, De Franceschi M, Fuchs C, Bastianini S, Viggiano R, Lupori L, Mazziotti R, Medici
696 G, Lo Martire V, Ren E, Rimondini R, Zoccoli G, Bartesaghi R, Pizzorusso T, Ciani E (2018)
697 CDKL5 protein substitution therapy rescues neurological phenotypes of a mouse model of
698 CDKL5 disorder. Hum Mol Genet. 27 (9): 1572-1592.

699 Trazzi S, Fuchs C, Viggiano R, De Franceschi M, Valli E, Jedynak P, Hansen FK, Perini G,
700 Rimondini R, Kurz T, Bartesaghi R, Ciani E (2016) HDAC4: a key factor underlying brain
701 developmental alterations in CDKL5 disorder. Hum Mol Genet. 25 (18): 3887-3907.

702 Vigli D, Rusconi L, Valenti D, La Montanara P, Cosentino L, Lacivita E, Leopoldo M,
703 Amendola E, Gross C, Landsberger N, Laviola G, Kilstrup-Nielsen C, Vacca RA, De Filippis
704 B (2018) Rescue of prepulse inhibition deficit and brain mitochondrial dysfunction by
705 pharmacological stimulation of the central serotonin receptor 7 in a mouse model of CDKL5
706 Deficiency Disorder. Neuropharmacology. 144:104-114.

707 Wang IT, Allen M, Goffin D, Zhu X, Fairless AH, Brodkin ES, Siegel SJ, Marsh ED, Blendy
708 JA, Zhou Z (2012) Loss of CDKL5 disrupts kinome profile and event-related potentials leading
709 to autistic-like phenotypes in mice. Proc Natl Acad Sci U S A 109 (52): 21516-21.

710 Weaving LS, Christodoulou J, Williamson SL, Friend KL, McKenzie OL, Archer H, Evans J,

711 Clarke A, Pelka GJ, Tam PP, Watson C, Lahooti H, Ellaway CJ, Bennetts B, Leonard H, Gécz
712 J (2004) Mutations of CDKL5 cause a severe neurodevelopmental disorder with infantile
713 spasms and mental retardation. Am J Hum Genet. 75 (6): 1079-93.

714 Whitmire CJ, Stanley GB (2016) Rapid sensory adaptation redux: a circuit perspective.
715 Neuron. 92 (2): 298-315.

716 Wimmer VC, Broser PJ, Kuner T, Bruno RM (2010) Experience-induced plasticity of
717 thalamocortical axons in both juveniles and adults. J Comp Neurol. 518 (22): 4629-48.

718 Yang G, Pan F, Gan WB (2009) Stably maintained dendritic spines are associated with
719 lifelong memories. Nature 462 (7275): 920-4.

720 Yennawar M, White RS, Jensen FE (2019) AMPA receptor dysregulation and therapeutic
721 interventions in a mouse model of CDKL5 Deficiency Disorder. J Neurosci. pii: 2041-18.

722 Yu X, Chung S, Chen DY, Wang S, Dodd SJ, Walters JR, Isaac JT, Koretsky AP (2012)
723 Thalamocortical inputs show post-critical-period plasticity. Neuron. 74 (4): 731-42.

724 Zerbi V, Ielacqua GD, Markicevic M, Haberl MG, Ellisman MH, A-Bhaskaran A, Frick A,
725 Rudin M, Wenderoth N (2018) Dysfunctional autism risk genes cause circuit-specific
726 connectivity deficits with distinct developmental trajectories. Cereb Cortex. 28 (7): 2495-2506.

727 Zhang Y, Bonnan A, Bony G, Ferezou I, Pietropaolo S, Ginger M, Sans N, Rossier J, Oostra
728 B, LeMasson G, Frick A (2014) Dendritic channelopathies contribute to neocortical and sensory
729 hyperexcitability in Fmr1(-/y) mice. Nat Neurosci. 17 (12): 1701-9.

730 Zhang Y, Matt L, Patriarchi T, Malik ZA, Chowdhury D, Park DK, Renieri A, Ames JB, Hell
731 JW (2014) Capping of the N-terminus of PSD-95 by calmodulin triggers its postsynaptic
732 release. EMBO J. 33 (12): 1341-53.

733 Zhu YC, Li D, Wang L, Lu B, Zheng J, Zhao SL, Zeng R, Xiong ZQ (2013) Palmitoylation-
734 dependent CDKL5-PSD-95 interaction regulates synaptic targeting of CDKL5 and dendritic
735 spine development. Proc Natl Acad Sci U S A 110 (22): 9118-23.

FIGURE LEGENDS

Figure 1 EE promotes an enhancement of thalamo-cortical connectivity.

A, Representative micrographs acquired in the neuropil of BC layer IV, illustrating VGluT2-positive immunofluorescence (red) and NeuroTrace fluorescent Nissl labeling (green) from Cdkl5$^{+/y}$ and Cdkl5$^{-/y}$ mice exposed to standard (SE) and enriched environment (EE) (scale bar 5 µm). **B**, Quantitative analysis of the density of VGluT2-positive puncta shows a significant increase in both WT and Cdkl5$^{-/y}$ mice exposed to EE compared to corresponding SE groups (n = 8). **C**, Representative confocal micrographs of BC layer IV neuropil showing immunofluorescence staining for VGluT1 from Cdkl5$^{+/y}$ and Cdkl5$^{-/y}$ mice kept in standard (SE) and enriched environment (EE) (scale bar 5 µm). **D**, Quantification of the density of VGluT1^{+} puncta revealed no overall changes in the number of intra-cortical excitatory terminals between WT and Cdkl5 mutants both under standard and enriched conditions (n = 4-5). Statistical analyses: two-way ANOVA followed by Post hoc Fisher's LSD test, * $p < 0.05$.

Figure 2 EE corrects the thalamo-cortical and the intra-cortical connectivity defects in Cdkl5$^{-/y}$ mice.

A, Representative confocal micrographs of BC layer IV neuropil showing immunofluorescence staining for VGluT2 (red) and Homer (green) from Cdkl5$^{+/y}$ and Cdkl5$^{-/y}$ mice kept in standard (SE) and enriched environment (EE) (scale bar 5 µm). **B**, Quantitative analysis of the number of VGluT2^{+} terminals juxtaposed to Homer^{+} puncta indicates that EE corrects the reduced VGluT2-Homer apposition index observed in Cdkl5$^{-/y}$ mice under standard conditions (n = 6). **C**, Distribution of VGluT2^{+} terminals based on the number of juxtaposed Homer^{+} puncta. Note that under SE KO mice exhibit a higher percentage of solitary VGluT2^{+} terminals (i.e. not facing Homer^{+} puncta; indicated by white arrowheads in **A**), as well as a lower percentage of VGluT2^{+} puncta with two Homer^{+} partners, whereas these differences are not observed following EE (n = 6). **D**, Representative confocal micrographs of BC layer IV neuropil showing VGluT1 (red) and Homer (green) puncta from Cdkl5$^{+/y}$ and Cdkl5$^{-/y}$ mice housed in standard (SE) and enriched environment (EE) (scale bar 5 µm). **E**, The analysis of the number of VGluT1-Homer appositions shows that EE exposure restores the reduction in cortico-cortical synapses found in Cdkl5$^{-/y}$ mice under SE (n = 5). **F**, The distribution analysis of VGluT1^{+} terminals, based on the number of juxtaposed Homer^{+} puncta, revealed that SE-mutant mice display a higher percentage of VGluT1^{+} terminals lacking a Homer^{+} postsynaptic partner as well as a lower percentage of VGluT1^{+} puncta with two Homer^{+} counterparts; these differences

were abolished by EE (n = 5). Statistical analyses: two-way ANOVA followed by Post hoc Fisher's LSD test, * $p < 0.05$, ** $p < 0.01$.

Figure 3 No effects of EE on inhibitory GABAergic connectivity in layer IV of the BC.
A, Examples of $VGAT^+$ puncta contacting the somata of layer IV pyramidal neurons in BC from WT and Cdkl5-KO mice (scale bar 5 µm). **B,** Quantitative analysis shows no changes in the density of inhibitory varicosities between WT and mutant mice (n = 5). **C, D,** Representative images acquired in the neuropil of BC layer IV depicting $VGAT^+$ staining (**C**) (scale bar 5 µm) and quantitative analysis (**D**) showing no differences in the density of the GABAergic terminals irrespective of both genotype and environmental exposure (n = 5). Statistical analysis: two-way ANOVA followed by Post hoc Fisher's LSD test.

Figure 4 Cdkl5-KO mice exhibit abnormal responses to repeated whisker stimulation.
A, Experimental timeline of the whisker nuisance task (WNT). **B,** Graph showing the total WN scores across trials (n = 9; statistical analysis: two-way ANOVA followed by Post hoc Fisher's LSD test, ** $p < 0.01$). **C-G**, WN scores recorded for each animal during trials (**C**) and average WN scores assigned to animals during trials (**D-G**) (n = 9; statistical analysis: two-way ANOVA with RM followed by Post hoc Fisher's LSD test, * $p < 0.05$, ** $p < 0.01$ between groups (**C-G**) and trial 1 vs trial 3 within groups (**D-G**). **H-L**, Mean score across trials for each of the five behavioural parameters (fearful behaviour, stance, response to stick, evasion, grooming) monitored during the WNT (n = 9; statistical analysis: two-way ANOVA followed by Post hoc Fisher's LSD test, * $p < 0.05$, ** $p < 0.01$, *** $p < 0.001$).

Figure 5 Cdkl5-KO mice exhibit reduced cortical activation to repeated whisker stimulation.
A, B, Representative examples of c-Fos staining in BC of WT and mutant mice housed in standard and enriched environment (scale bar 50 mm) (**A**) and quantification of the density of $c\text{-}Fos^+$ cells (**B**) (n = 6-8; statistical analysis: two-way ANOVA followed by Post hoc Fisher's LSD test, * $p < 0.05$, ** $p < 0.01$, *** $p < 0.001$).

800 **Table 1. Mean ± SEM values for each statistical analysis.**

801

Figure			SE		EE	
			Cdkl5$^{+/y}$	Cdkl5$^{-/y}$	Cdkl5$^{+/y}$	Cdkl5$^{-/y}$
Fig 1B	VGluT2$^+$ puncta density (puncta/μm^2)		0.123 ± 0.01	0.11 ± 0.01	0.174 ± 0.02	0.162 ± 0.02
Fig 1D	VGluT1$^+$ puncta density (puncta/μm^2)		0.136 ± 0.01	0.134 ± 0.00	0.131 ±0.01	0.149 ±0.01
Fig 2B	VGluT2$^+$ - Homer$^+$ appositions density (puncta/μm^2)		0.117 ± 0.01	0.093 ± 0.01	0.139 ± 0.01	0.120 ±0.01
Fig 2C	VGluT2$^+$ puncta distribution (%)	0 Homer$^+$	26.50 ± 2.12	35 ± 0.84	25 ± 3.74	27 ± 1.38
		1 Homer$^+$	40.67 ± 0.99	42 ± 0.84	39.17 ± 2.64	43.20 ± 1.16
		2 Homer$^+$	27 ± 2.52	20 ± 0.95	28.83 ± 2.59	23.60 ± 0.4
		>2 Homer$^+$	5.67 ± 0.8	3.3 ± 1.2	6.83 ± 1.89	6 ± 1.05
Fig 2E	VGluT1$^+$ - Homer$^+$ appositions density (puncta/μm^2)		0.133 ± 0.02	0.10 ± 0.01	0.12 ± 0.01	0.13 ± 0.01
Fig 2F	VGluT1$^+$ puncta distribution (%)	0 Homer$^+$	24.51 ± 3.53	36.94 ± 2.84	26.08 ± 1.39	29.96 ± 2.82
		1 Homer$^+$	54.26 ± 3.07	52.17 ± 2.33	56.14 ± 4.99	51.09 ± 1.76
		≥2 Homer$^+$	21.22 ± 3.64	10.9 ± 2.36	17.79 ± 4.38	18.95 ± 2.20
Fig 3B	VGAT$^+$ puncta density on pyramidal neurons (puncta/μm)		0.54 ± 0.02	0.52 ± 0.02	0.50 ± 0.03	0.52 ± 0.01
Fig 3D	VGAT$^+$ puncta density (puncta/μm^2)		0.13 ± 0.00	0.13 ± 0.00	0.13 ± 0.00	0.13 ± 0.00
Fig 4B	WNT score	Across trials	3.75 ± 0.27	3.38 ± 0.14	4.16 ± 0.20	3.73 ± 0.14
Fig 4C-G		Trial 1	4.19 ± 0.27	3.09 ± 0.19	4.17 ± 0.21	3.14 ± 0.21
		Trial 2	3.75 ± 0.43	3.54 ± 0.17	4.25 ± 0.33	3.77 ± 0.22
		Trial 3	3.31 ± 0.37	3.50 ± 0.19	4.08 ± 0.44	4.04 ± 0.26
Fig 4H	Fearful behaviour		0.50 ± 0.11	0.11 ± 0.05	0.89 ± 0.21	0.59 ± 0.16
Fig 4J	Stance		1.45 ± 0.19	0.58 ± 0.14	1.69 ± 0.12	1.27 ± 0.18
Fig 4J	Stick Response		0.62 ± 0.14	1.54 ± 0.17	0.86 ± 0.26	0.91 ± 0.22
Fig 4K	Evasion		1.07 ± 0.18	0.71 ± 0.19	0.57 ± 0.26	0.39 ± 0.18
Fig 4L	Grooming		0.10 ± 0.07	0.44 ± 0.10	0.33 ± 0.12	0.49 ± 0.11
Fig 5B	cFos$^+$ cells density (cells/mm^2)	Layer I	145.7 ± 72.44	44.32 ± 25.52	34.89 ± 7.37	64.69 ± 14.10
		II-III	470.4 ± 142.9	304.9 ± 69.15	178.0 ± 23.87	450.9 ± 63.85
		IV	598.8 ± 157.1	299.1 ± 77.42	166.7 ± 45.72	812.6 ± 183.3
		V	284.1 ± 97.47	147.0 ± 49.15	103.2 ± 11.67	314.9 ± 50.20
		VI	342.4 ± 75.32	242.6 ± 81.03	172.8 ± 34.82	499.5 ± 81.23
		I-VI	368.3 ± 102.5	207.6 ± 52.35	131.1 ± 20.12	428.5 ± 72.10

802

803 **Table 2. Statistical tests and statistical power yielded**

804

Figure		Statistical Analysis		Power	
Fig 1B	VGluT2$^+$ puncta density	Two-way ANOVA		Genotype (G) Environment Exposure (E) G x E	0,14 0,95 0,05
Fig 1D	VGluT1$^+$ puncta density	Two-way ANOVA		G 0,15; E 0,1; G x E 0,21	
Fig 2B	VGluT2$^+$ - Homer$^+$ appositions density	Two-way ANOVA		G 0,84; E 0,93; G x E 0,06	
Fig 2C	VGluT2$^+$ puncta distribution	Two-way ANOVA	0 Homer$^+$ 1 Homer$^+$ 2 Homer$^+$ >2 Homer$^+$	G 0,6; E 0,51; G x E 0,28 G 0,38; E 0,05; G x E 0,13 G 0,87; E 0,28; G x E 0,07 G 0,25; E 0,34; G x E 0,1	
Fig 2E	VGluT1$^+$ - Homer$^+$ appositions density	Two-way ANOVA		G 0,16; E 0,18; G x E 0,65	
Fig 2F	VGluT1$^+$ puncta distribution	Two-way ANOVA	0 Homer$^+$ 1 Homer$^+$ ≥2 Homer$^+$	G 0,86; E 0,17; G x E 0,36 G 0,23; E 0,05; G x E 0,08 G 0,35; E 0,12; G x E 0,5	
Fig 3B	VGAT$^+$ puncta density on pyramidal neurons	Two-way ANOVA		G 0,05; E 0,14; G x E 0,12	
Fig 3D	VGAT$^+$ puncta density	Two-way ANOVA		G 0,1; E 0,06; G x E 0,05	
Fig 4B	WNT score	Two-way ANOVA		G 0,57; E 0,49; G x E 0,08	
Fig 4C-G	WNT score during trials	Two-way ANOVA with RM		G 0,87; E 0,73; G x E 0,19; Trials (T) 0,14; T x G 0,66 T x E 0,36; TxGxE 0,08	
Fig 4H	Fearful behaviour	Two-way ANOVA		G 0,73; E 0,9; G x E 0,06	
Fig 4I	Stance	Two-way ANOVA		G 0,99; E 0,8; G x E 0,27	
Fig 4J	Stick response	Two-way ANOVA		G 0,65; E 0,16; G x E 0,56	
Fig 4K	Evasion	Two-way ANOVA		G 0,13; E 0,8; G x E 0,2	
Fig 4L	Grooming	Two-way ANOVA		G 0,48; E 0,32; G x E 0,19	
Fig 4N	cFos$^+$ cells density	Two-way ANOVA	Layer I II-III IV V VI I-VI	G 0,17; E 0,25; G x E 0,45 G 0,1; E 0,14; G x E 0,45 G 0,21; E 0,06; G x E 0,88 G 0,1; E 0,05; G x E 0,84 G 0,33; E 0,09; G x E 0,82 G 0,16; E 0,05; G x E 0,89	

805

806

Figure 1

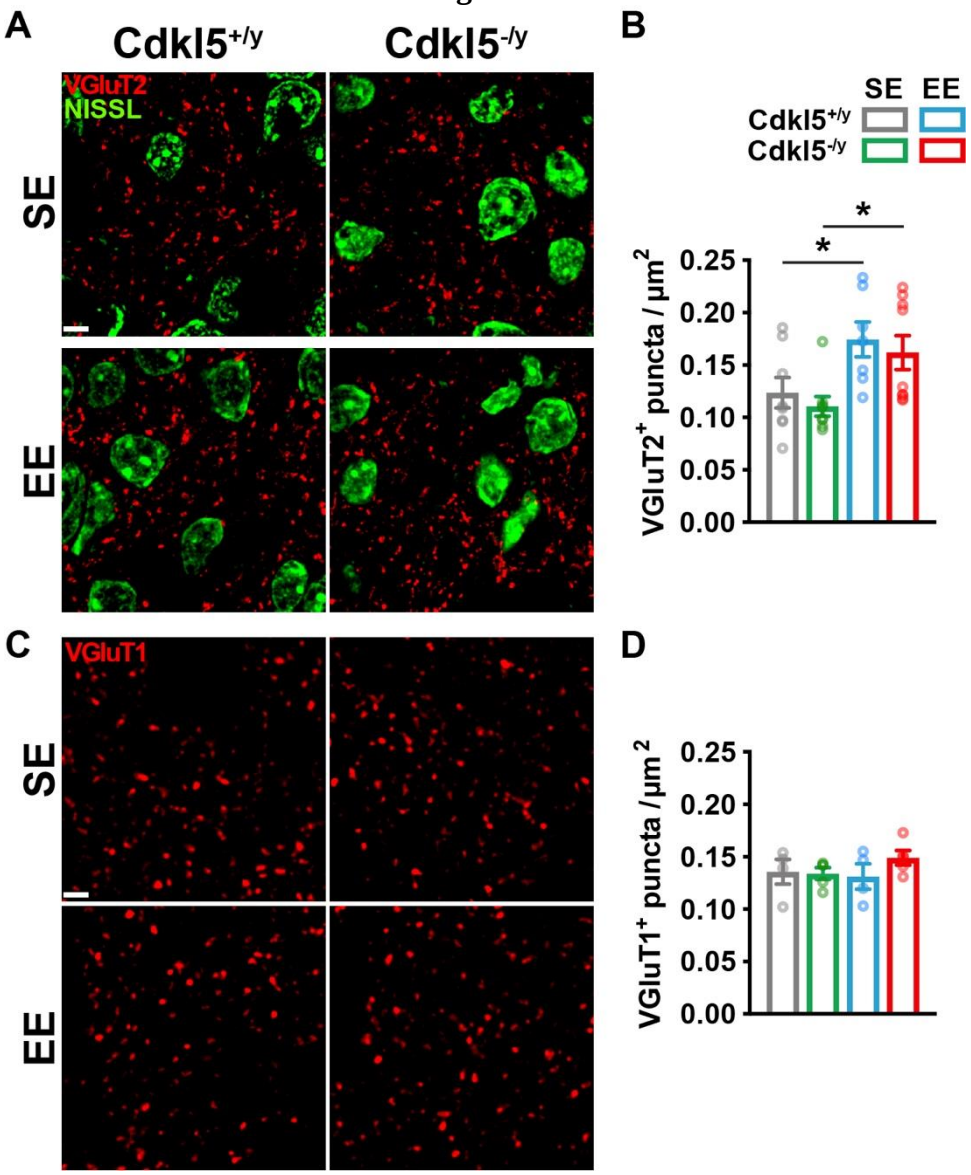

807
808

809

Figure 2

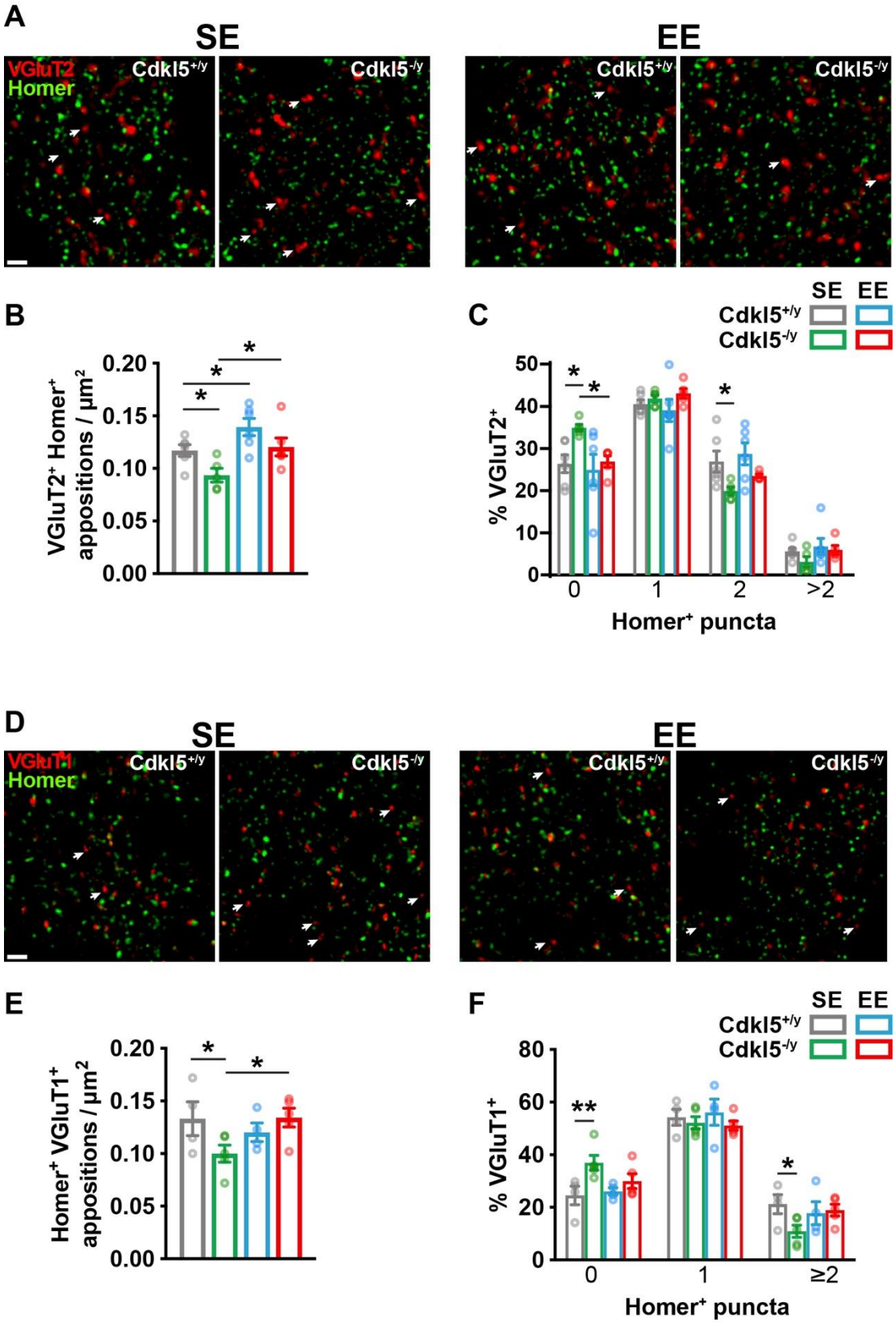

810

811

Figure 3

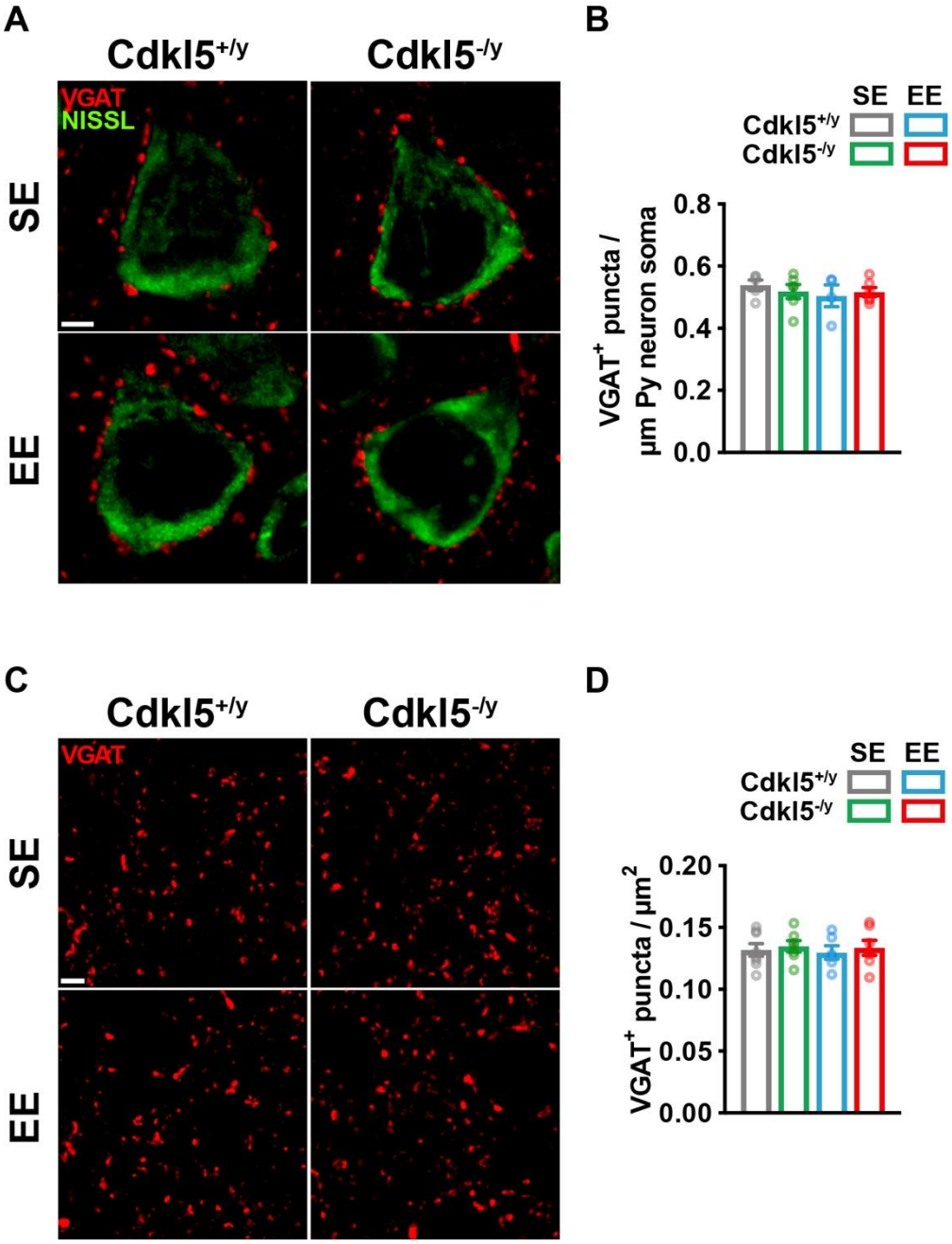
A
Cdkl5+/y
Cdkl5-/y
VGAT
NISSL
SE
EE
B
SE
EE
Cdkl5+/y
Cdkl5-/y
VGAT+ puncta / µm Py neuron soma
0.8
0.6
0.4
0.2
0.0
C
Cdkl5+/y
Cdkl5-/y
VGAT
SE
EE
D
SE
EE
Cdkl5+/y
Cdkl5-/y
VGAT+ puncta / µm2
0.20
0.15
0.10
0.05
0.00

Figure 4

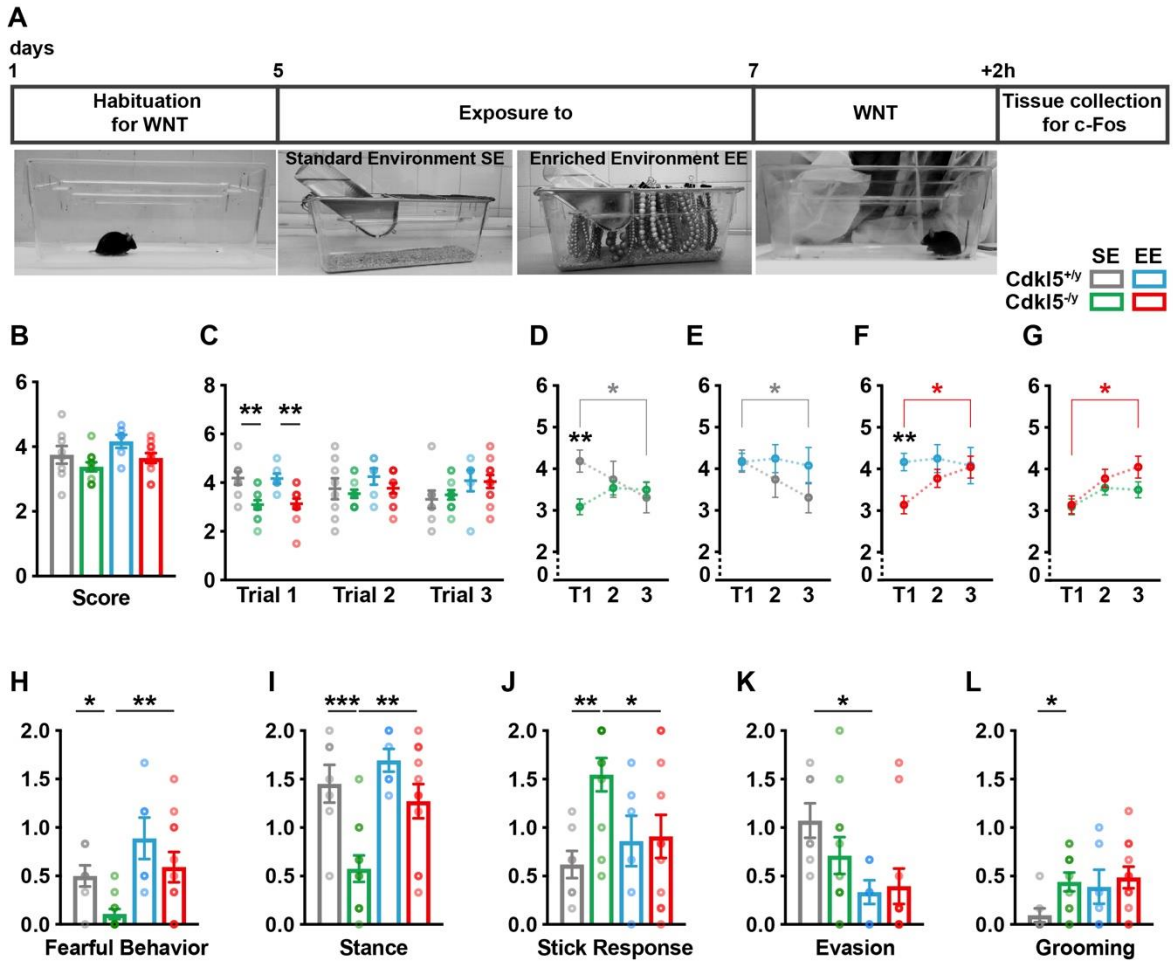
A
days
1
5
7
+2h
Habituation for WNT
Exposure to
WNT
Tissue collection for c-Fos
Standard Environment SE
Enriched Environment EE
SE EE
Cdkl5+/y
Cdkl5-/y
B
Score
C
Trial 1
Trial 2
Trial 3
D
E
F
G
T1 2 3
H
Fearful Behavior
I
Stance
J
Stick Response
K
Evasion
L
Grooming

Figure 5

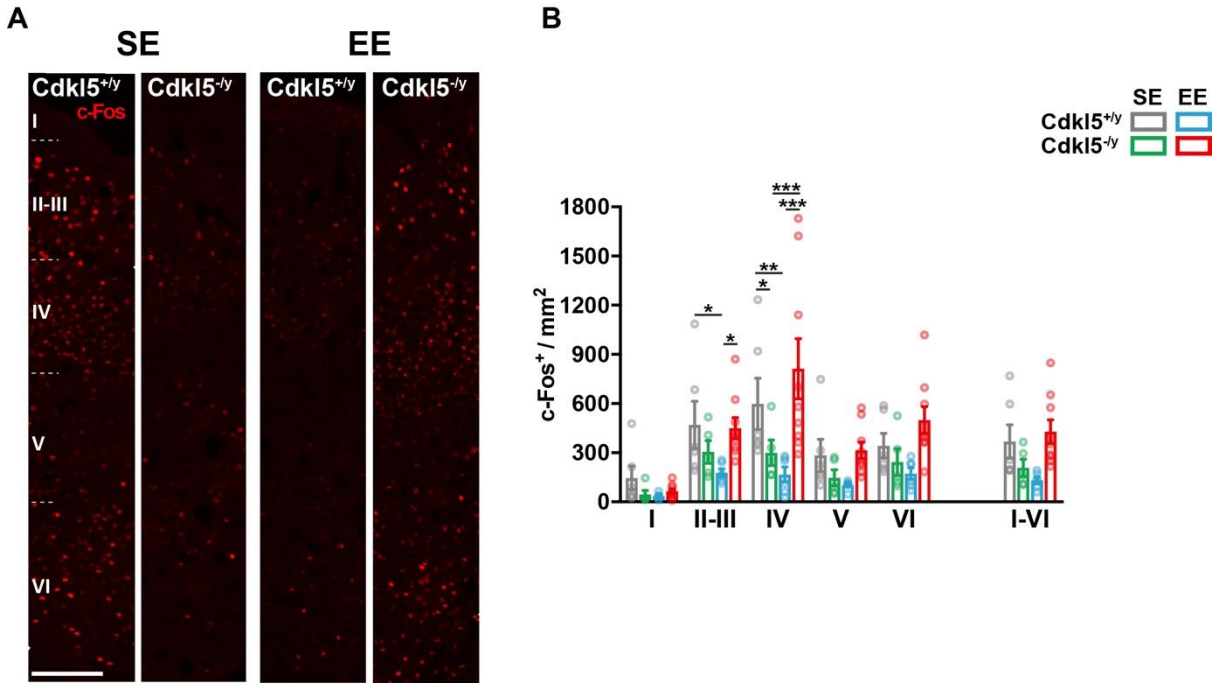
A
SE
EE
Cdkl5+/y
Cdkl5-/y
Cdkl5+/y
Cdkl5-/y
c-Fos
I
II-III
IV
V
VI
B
SE
EE
Cdkl5+/y
Cdkl5-/y
c-Fos+ / mm2
1800
1500
1200
900
600
300
0
I
II-III
IV
V
VI
I-VI